J Eng Math (2007) 58:317–337
DOI 10.1007/s10665-006-9128-0

ORIGINAL PAPER

Penetration of flexural waves through a periodically constrained thin elastic plate in *vacuo* and floating on water

D. V. Evans · R. Porter

Received: 6 February 2006 / Accepted: 15 December 2006 / Published online: 1 March 2007

Abstract The subject of this paper, the scattering of flexural waves by constrained elastic plates floating on water is relatively new and not an area that Professor Newman has worked in, as far as the authors are aware. However, in two respects there are connections to his own work. The first is the reference to his work with H. Maniar on the exciting forces on the elements of a long line of fixed vertical bottom-mounted cylinders in waves. In their paper (J Fluid Mech 339 (1997) 309–329) they pointed out the remarkable connection between the large forces on cylinders near the centre of the array at frequencies close to certain trapped-mode frequencies, which had been discovered earlier, and showed that there was another type of previously unknown trapped mode, which gave rise to large forces. In Sect. 6 of this paper the ideas described by Maniar and Newman are returned to and it is shown how the phenomenon of large forces is related to trapped, or standing Rayleigh–Bloch waves, in the present context of elastic waves. But there is a more general way in which the paper relates to Professor Newman and that is in the flavour and style of the mathematics that are employed. Thus extensive use has been made of classical mathematical methods including integral-transform techniques, complex-function theory and the use of special functions in a manner which reflects that used by Professor Newman in many of his important papers on ship hydrodynamics and related fields.

Keywords Flexural waves · Kirchhoff plate theory · Periodic arrays · Trapping

1 Introduction

In recent years there has been considerable interest in problems involving very large floating structures for a variety of practical reasons. One of these was the possibility of designing a massive floating concrete runway offshore. Such a structure would inevitably bend under the influence of wave action and this prompted a whole new set of challenging interaction problems involving the structure and the supporting body of water. A wide range of references to such problems can be found in [1].

D. V. Evans · R. Porter
School of Mathematics, University of Bristol, Bristol BS8 1TW, UK
e-mail: d.v.evans@bris.ac.uk

R. Porter (✉)
e-mail: richard.porter@bris.ac.uk

In this paper we consider a specific set of problems which appear to have intrinsic interest in their own right, whilst also being of relevance to applications. The free surface of a body of water of depth h extending indefinitely in both horizontal directions is covered by a uniform thin elastic plate. It is known that flexural-gravity waves can propagate through the plate with a wavenumber determined from a dispersion relation obtained through the coupling of the plate and the fluid motion. In practical applications large floating elastic plates may be secured by a large number of fixed vertical cylindrical columns extending throughout the depth of water. Other possibilities might include tethering the structure to the sea bed using a large number of moorings.

In the simplest model the region of contact between the top of the columns and the underside of the plate would be fixed and a problem of practical interest would be to determine the wave forces at those regions due to a prescribed incoming wave field. For a theoretical single supporting column the wave-induced flexure would create a force which attempts to break the contact with the support and it can confidently be presumed that such a force would be proportional to the incident wave height. In practice, large numbers of supporting columns would be needed and design considerations would dictate that they be placed in some regular, perhaps rectangular pattern.

Now the prediction of wave forces on each region of contact is clearly less easy, since resonant interactions between neighbouring supports is possible. A vivid illustration in a related context is provided by Maniar and Newman [2] who computed the horizontal wave-exciting forces on a linear regular array of a hundred identical vertical bottom-mounted circular cylinders in finite-depth water. They showed that at two particular incident wave frequencies the force on the cylinders near the centre of the array could be over 30 times the force on a cylinder in isolation in the same wave field. One of these frequencies coincided with the so-called trapped-mode frequencies discovered by Callan et al. [3] for a single circular cylinder in a channel in a wave tank of width the same as the spacing between adjacent cylinders in the linear array of cylinders, when a Neumann condition, representing no-flow through the tank walls, is applied. The second frequency for which large forces occurred led to the discovery of a trapped mode in which a Dirichlet condition is satisfied on the walls of the tank. See, for example [4]. Again, Evans and Porter [5] showed that in the water-wave context, vertical bottom-mounted circular cylinders now arranged with regular spacing on a circle, could experience large wave-exciting forces. In particular, for just four cylinders with centres at the vertices of a square, the horizontal exciting force on each of the cylinders could be as high as 54 times the force on just one of them in isolation, when the spacing between the cylinders was reduced to half the diameter of the cylinders, but the effect disappeared when the symmetry was broken by slightly increasing the size of one of the cylinders, at the same spacing.

We expect similar effects in the problems discussed here, but for the very large number of supports which would be required to secure the floating platform suggests that we are dealing with a two-dimensional lattice problem similar to that which arises in solid-state physics. See, for example [6]. Thus, a regular two-dimensional array of circular contact regions between supports and plate constitutes a lattice which, if assumed to extend indefinitely in two horizontal directions, permits flexural waves only in certain directions, depending on the value of the wavenumber. This is a substantial problem in its own right on which the authors have made considerable progress and which will be published separately.

It might be expected that a wave approaching a *finite* lattice of supports in directions prohibited by the *infinite* lattice theory, would create large forces at the regions of attachment, since the wave energy would not be able to escape easily, once inside the lattice.

It is clear from the above that the information on infinite two-dimensional lattices will be invaluable in predicting the design forces at regions of contact between columns and floating platforms in finite two-dimensional arrays. However, even assuming small amplitude waves, the linearised boundary-value problem is formidable and certain assumptions need to be made to make progress without compromising the qualitative validity of the results. First, the columns are (reasonably) assumed to have diameters small compared to the flexural wavelengths in the elastic plate so that: (a) the effect of the columns beneath the plate on the wave field is negligible and (b) the regions of contact between the top of the columns and

the plate are assumed to be points which considerably simplifies the conditions which are satisfied there. A similar assumption has been made to good effect in developing the so-called "point absorber" theory for wave energy absorbers (see, for example [7]). With these assumptions, considerable progress can be made using a Green function located at the point on the plate over water and the wave field can be expressed as appropriate sums of such functions at each of the contact points between the columns and plate. Because of the high-order nature of the boundary condition on the plate, expressed in terms of the velocity potential defined throughout the fluid, the Green function itself is bounded at the contact points and the required conditions there are easily satisfied.

We concentrate initially on a much simpler problem, which has all the key properties of the full problem, namely a thin uniform elastic plate of infinite extent in *vacuo* which is pinned at a number of distinct points which may form a lattice. The only difference between the full problem and this model is in the simpler Green function which, when located at the origin, is now only a function of kr, where r is the radial distance in the plane from the origin and k is the wavenumber for flexural waves in the infinite plate, given by $k^4 = m\omega^2/D$. Here ω is the assumed angular frequency of motion, D is the bending stiffness of the plate and m its mass per unit area. This simpler problem is of considerable interest in its own right, modelling as it does the riveting of elastic plates in *vacuo*. Some early results for this model can be found in [8].

We must emphasize that we expect all of the qualitative behaviour predicted by this simpler model to be reflected in the full model which only requires the use of the more general Green function incorporating the effect of the water under the plate. This claim can certainly be supported for high-frequency short-wavelength wave motions in which scalings laws presented later in Sect. 8 show that the effect of the fluid loading under the elastic plate is negligible. For more realistic longer waves of lower frequencies, this is shown no longer to be the case.

Reverting to the simpler problem then, the assumption of a pinned point on a thin elastic plate needs some discussion. Suppose that the region of contact is a small circle of radius ϵ on which the plate is clamped. The boundary condition to be satisfied on the circumference according to thin-plate theory is the vanishing of displacement and its radial derivative on $r = \epsilon$; it is a simple matter to solve for the scattering of an incident waves in the plate by such a clamped region. The solution is given by Norris and Vermula [9] who also show that as $\epsilon \to 0$ the solution is given in terms of a multiple of the Green function for the thin plate at $r = 0$, the constant being chosen to ensure that the *total* displacement, including the incident wave, vanishes on $r = 0$. But in the course of taking the limit $\epsilon \to 0$, the second condition on the vanishing of the radial derivative at $r = 0$ has to be relaxed. We shall adopt this assumption throughout, namely that the single condition to be satisfied at a pinned point of the plate is the vanishing of the normal displacement.

We start in Sect. 2 by introducing the governing equations for wave motion on a thin elastic plate in *vacuo* and introduce some basic ideas by considering the simple problem of the scattering of plane flexural waves by a single point, generalising the case where it is pinned to the case where it is constrained to move by an impedance condition which includes the effects of a concentrated-mass loading, a spring term and damping. In Sect. 3, a similar problem involving an arbitrary number of such points is considered, and near resonance is discussed for a circular arrangement of points extending to infinity. In Sects. 4–6, the focus is placed on either one or two rows of periodically constrained points. First, the scattering of a plane wave by a single infinite periodic array is considered and it is proved that there always exists a frequency for which there is total reflection of incident-wave energy. This property is used to consider trapping modes between two such arrays which have the appropriate spacing between them. In Sect. 6, conditions for the existence of Rayleigh–Bloch waves along the periodic array are proved. It is shown how the presence of a trapped mode or a Rayleigh–Bloch solution affects the solution in the scattering by a finite number of periods in the array.

In Sect. 7, we derive the corresponding formulation for the scattering by constrained points over water. Although more complicated, it is illustrated how all the problems considered in Sects. 2–6 can be repeated without any additional conceptual difficulty.

2 Some basic ideas: scattering by a single point

In its equilibrium position the thin elastic plate occupies the x–y plane and when excited by an incident wave field, undergoes a displacement normal to itself of the form $\Re\mathrm{e}\{u(\mathbf{r})\mathrm{e}^{-\mathrm{i}\omega t}\}$ where ω is the radian frequency of the incident excitation, and $\mathbf{r} = (x, y) = (r\cos\theta, r\sin\theta)$. Under classical Kirchhoff thin-plate theory $u(\mathbf{r})$ satisfies the equation of motion

$$D(\Delta^2 - k^4)u(\mathbf{r}) = 0, \quad -\infty < x, y < \infty \tag{2.1}$$

in the absence of external forces. Here, $\Delta = \partial^2/\partial x^2 + \partial^2/\partial y^2$ and $k^4 = m\omega^2/D$ where $D = Ed^3/12(1-\nu^2)$ with E Young's modulus, d the plate thickness, m the mass per unit area of the plate and ν is Poisson's ratio.

A solution of (2.1) describing a long-crested incident wave making an angle ψ with the positive x-axis is

$$u_i(\mathbf{r}) = \mathrm{e}^{\mathrm{i}k(x\cos\psi + y\sin\psi)} = \mathrm{e}^{\mathrm{i}kr\cos(\theta-\psi)} \tag{2.2}$$

and a fundamental Green function describing a time harmonic point force of strength D is given by

$$g(\mathbf{r};\mathbf{r}') = C\{H_0(k\rho) - H_0(\mathrm{i}k\rho)\}, \tag{2.3}$$

where $C = \mathrm{i}/8k^2$, $\rho = |\mathbf{r} - \mathbf{r}'|$, $\mathbf{r}' = (x', y')$ and $H_0(x) \equiv H_0^{(1)}(x)$ is the Hankel function of the first kind of order zero. Here, $g(\mathbf{r};\mathbf{r}')$ satisfies

$$(\Delta^2 - k^4)g(\mathbf{r};\mathbf{r}') = \delta(\mathbf{r} - \mathbf{r}') \tag{2.4}$$

and is outgoing for $\rho \to \infty$. The expression in (2.3) is well-known and can easily be derived using transform methods. A useful alternative formula is

$$g(\mathbf{r};\mathbf{r}') \equiv g(x - x', y - y') = \frac{C}{\pi\mathrm{i}}\int_{-\infty}^{\infty} \mathrm{e}^{\mathrm{i}k(x-x')t}\left(\frac{\mathrm{e}^{-k\lambda|y-y'|}}{\lambda} - \frac{\mathrm{e}^{-k\gamma|y-y'|}}{\gamma}\right)\mathrm{d}t, \tag{2.5}$$

where

$$\lambda = \begin{cases} (t^2-1)^{1/2}, & |t| \geq 1, \\ -i(1-t^2)^{1/2}, & |t| < 1, \end{cases} \quad \text{and} \quad \gamma = (1+t^2)^{1/2}. \tag{2.6}$$

An important property of $g(\mathbf{r};\mathbf{r}')$ is that it is bounded as $\mathbf{r} \to \mathbf{r}'$. From (2.3), it can be shown

$$g(\mathbf{r};\mathbf{r}') \sim C + \frac{\rho^2\log\rho}{8\pi} + O(\rho^2), \quad \rho \to 0, \tag{2.7}$$

whilst $\partial g/\partial\rho \to 0$ as $\rho \to 0$. This follows because g satisfies a fourth-order differential equation in contrast to the Green function for the Helmholtz equation describing small acoustic vibrations or the normal displacement of a taut membrane which is given by the first term on the right-hand side of (2.3) and which is logarithmically singular as $\rho \to 0$.

This boundedness property of g means that it can be used to solve a variety of interesting problems. The simplest is when the elastic plate is pinned at a single point, the origin, in the presence of an incident plane wave (2.2), satisfying $u_i(0,0) = 1$, when the solution is

$$u(\mathbf{r}) = u_i(\mathbf{r}) - C^{-1}g(\mathbf{r};0,0) \tag{2.8}$$

which satisfies (2.1) everywhere, except at $\mathbf{r} = 0$ where $u(0,0) = 0$ as required, and the scattered wave is outgoing. From (2.8),

$$D(\Delta^2 - k^4)u(\mathbf{r}) = -(D/C)\delta(\mathbf{r}), \tag{2.9}$$

showing that the point force exerted at the origin is $-D/C$.

Notice that in contrast to the simple solution above, it is not possible to use the corresponding Green function to pin a membrane.

A simple extension of the single *pinned* point is to assume that there is an external point force acting which is proportional to the displacement of the point through an impedance coefficient, μD say. Then the solution (2.8) is replaced by

$$u(\mathbf{r}) = u_i(\mathbf{r}) + Ag(\mathbf{r}; 0, 0), \tag{2.10}$$

where $A = \mu u(0,0)$. Thus, $\mu u(0,0) = A = \mu u_i(0,0) + \mu AC$ whence

$$A = \mu/(1 - \mu C), \quad \text{and} \quad u(0,0) = 1/(1 - \mu C). \tag{2.11}$$

The case of a pinned origin is recovered from (2.11) by letting $\mu \to \infty$. In general we can assume

$$\mu D = M\omega^2 - \kappa - \mathrm{i}\omega\nu \tag{2.12}$$

where k and ν are spring and damping restoring forces and M is a concentrated point mass. The case $\nu \neq 0$ implies energy dissipation at the point, a complication which we shall overlook by setting $\nu = 0$. Non-dimensional quantities, $\widetilde{\mu}$ and $\widetilde{\kappa}$ which depend only on physical parameters and not on frequency come from noting the relation $k^4 = m\omega^2/D$, and writing

$$\mu = (4k^4a^2)\widetilde{\mu} - 4\widetilde{\kappa}/a^2, \qquad \text{where } \widetilde{\mu} = M/(4ma^2),\ \ \widetilde{\kappa} = \kappa a^2/4D,$$

having anticipated the introduction of a length scale, a, to the problem.

3 Extension to scattering by N arbitrary points

Suppose each of the points $\mathbf{r}_n$, $n = 1, 2, \ldots, N$ supports a mass, spring and damper described by an impedance μ_n, given by (2.12) in terms of M_n, κ_n and ν_n. The displacement everywhere is given by

$$u(\mathbf{r}) = u_i(\mathbf{r}) + \sum_{n=1}^{N} A_n g(\mathbf{r}; \mathbf{r}_n) \tag{3.1}$$

and

$$D(\Delta^2 - k^4)u(\mathbf{r}) = D\sum_{n=1}^{N} A_n \delta(\mathbf{r} - \mathbf{r}_n), \tag{3.2}$$

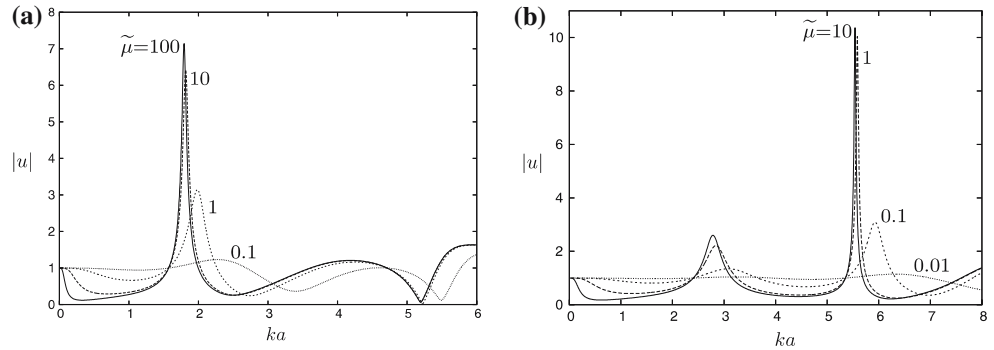

Fig. 1 Maximum displacement at the origin, $|u| = |u(0,0)|$ as ka varies for: (**a**) $N = 4$ points at $(\pm a, \pm a)$ with $\psi = 0°$; (**b**) $N = 8$ points at $(\pm a, 0)$, $(0, \pm a)$, $(\pm a/\sqrt{2}, \pm a/\sqrt{2})$ with $\psi = 0°$. Values of $\widetilde{\mu}$ are shown against curves and $\widetilde{\kappa} = 0$

showing that the external force at the nth pin, DA_n, satisfies $DA_n = \mu_n Du(\mathbf{r}_m)$, $n = 1, 2, \ldots, N$ whence from (3.1),

$$A_m = \mu_m u_i(\mathbf{r}_m) + \mu_m \sum_{n=1}^{\infty} A_n g(\mathbf{r}_m; \mathbf{r}_n), \quad m = 1, 2, \ldots, N \tag{3.3}$$

a system of algebraic equations for the constants A_n and hence the force at each point. The displacement is then

$$u(\mathbf{r}_n) = A_n/\mu_n.$$

The limiting case of N *pinned* points is recovered by letting $\mu_n \to \infty$ so that the A_n satisfy

$$\sum_{n=1}^{N} A_n g(\mathbf{r}_m; \mathbf{r}_n) = -u_i(\mathbf{r}_m), \quad m = 1, 2, \ldots, N \tag{3.4}$$

with the displacement everywhere still given by (3.1). We define non-dimensional coefficients with $\widetilde{A}_n = A_n/k^2$.

One particular configuration of points worthy of investigation is when the points are arranged at regular intervals on a circle.

In Fig. 1(a, b) we present results showing the maximum plate elevation (non-dimensionalised with respect to the incident wave amplitude) at the centre of $N = 4$ and $N = 8$ points for a range of values of $\widetilde{\mu}$ ($\widetilde{\kappa}$ is fixed at zero) as a function of wavenumber ka. The curves for $\widetilde{\mu} = 100$ and $\widetilde{\mu} = 10$ in Fig. 1(a, b) change only very slightly for larger values of $\widetilde{\mu}$ and therefore gives an indication of the response when the array of points is pinned. Thus the pinned array is the one which gives the largest response at the centre of the array, being close to ten times the incident wave amplitude in the two cases. As expected, reduction of the point mass loading on the plate (a decreased value of $\widetilde{\mu}$) leads to less resonance. It should be noted that, if both $\widetilde{\kappa}$ and $\widetilde{\mu}$ are non-zero but finite, there is an additional resonance in the system which is associated with the excitation of the mass/spring oscillators at each of the individual points. Such a resonance has an analogue in the study of freely floating bodies excited by incident waves, which also exhibit resonance which depends upon the added mass and radiation damping coefficients of the body (see [10, Sect. 6.18] for example). Consideration of the case when $\widetilde{\mu} = 0$ but $\widetilde{\kappa} \neq 0$, provides little added insight into this particular problem, needless to say that the limit $\widetilde{\kappa} \to \infty$ is equivalent to points that are pinned.

The nature of the resonance can be observed by plotting the maximum absolute value of the displacement $|u(\mathbf{r})|$ across the plate at the resonant frequencies for $N = 4$ and $N = 8$. This is done in Fig. 2(a, b)

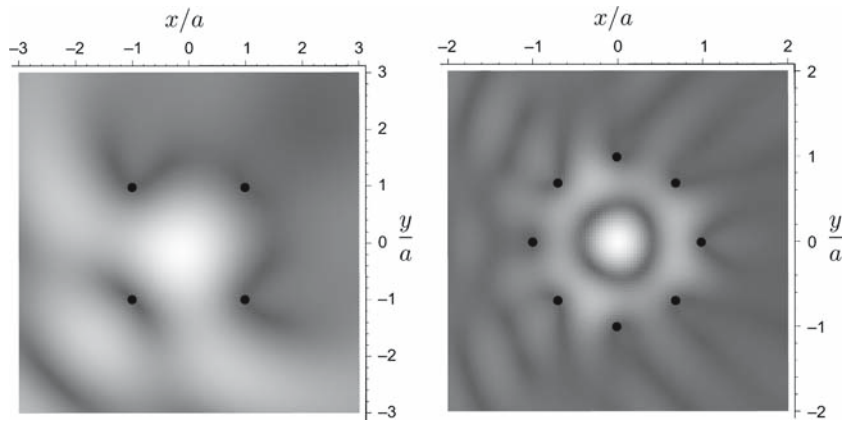

Fig. 2 Modulus of the wave amplitude, $|u(\mathbf{r})|$, with $\widetilde{\mu}^{-1} = 0$ (pinned points, shown as dots) and (**a**) $N = 4$ with $\psi = 45°$, $ka = 1.792$; (**b**) $N = 8$ with $\psi = 0°$, $ka = 5.5344$

where incident wave angles of 45° and 0° (respectively) have been used. Light to dark shading represents the transition from high to low amplitudes. The scale of the shading can be established with reference to Fig. 1, so that the lightest shading at the centre of each figure corresponds to amplitudes of approximately 7.5 and 10.5 in Fig. 7(a, b).

4 Scattering by an infinite array of identical equally spaced points

In general the scattering by N arbitrary points, each satisfying an impedance condition such as (3.3) with μ_n given by (2.12), requires the numerical solution of the $N \times N$ system (3.4). Whilst this is straightforward for any particular configuration, more light is shed on the scattering process by considering problems which permit further analytic progress. Such a problem is provided by the assumption that the incident wave field (2.2) is scattered by an infinite periodic array of points, each satisfying the same impedance relation,

$$A_n = \mu u(\mathbf{r}_n), \quad \text{where } \mathbf{r}_n = (na, 0), n \in \mathbb{Z} \tag{4.1}$$

and a is the spacing between adjacent points. Then the solution may be written

$$u(\mathbf{r}) = u_i(\mathbf{r}) + \sum_{n=-\infty}^{\infty} A_n g(\mathbf{r}; \mathbf{r}_n). \tag{4.2}$$

But it is clear from the periodicity that the only difference between successive values of A_n is the change in phase of the incident wave field from one point to the next. Thus $A_n = A_{n-1}\sigma$, where $\sigma = \mathrm{e}^{\mathrm{i}\beta a}$ and $\beta = k\cos\psi$ and so $A_n = \sigma^n A_0$. It follows that

$$A_0\sigma^m = \mu\sigma^m + \mu A_0 \sum_{n=-\infty}^{\infty} \sigma^n g((m-n)a, 0), \tag{4.3}$$

where we have re-introduced the abbreviation $g(\mathbf{r}; \mathbf{r}') = g(x - x', y - y')$ for convenience and, from (2.5),

$$g((m-n)a, 0) = \frac{C}{\pi\mathrm{i}} \int_{-\infty}^{\infty} \mathrm{e}^{\mathrm{i}k(m-n)ta} \left(\lambda^{-1}(t) - \gamma^{-1}(t)\right) \mathrm{d}t. \tag{4.4}$$

It follows, from (4.3) and (4.4) by redefining the summation variable, that

$$A_0 = \mu(1 + A_0 S), \quad \text{where } S = \sum_{n=-\infty}^{\infty} \sigma^{-n} g(na, 0) \tag{4.5}$$

and so

$$A_0 = \mu/(1 - \mu S), \quad \text{and} \quad u(na, 0) = \sigma^n/(1 - \mu S) \tag{4.6}$$

from (4.1). The problem is now solved completely, the entire field being given by (4.2), which nows reads as

$$u(\mathbf{r}) = u_i(\mathbf{r}) + u_s(\mathbf{r}), \quad \text{where } u_s(\mathbf{r}) = A_0 \sum_{n=-\infty}^{\infty} \sigma^n g(\mathbf{r}; na, 0). \tag{4.7}$$

To gain further insight into the solution, we need to consider the sum in (4.7) and also in the definition of S given by (4.5). To do this we make use of the Poisson formula

$$\sum_{n=-\infty}^{\infty} \int_{-\infty}^{\infty} \mathrm{e}^{\pm \mathrm{i}nu} F(u)\mathrm{d}u = 2\pi \sum_{n=-\infty}^{\infty} F(2\pi n) \tag{4.8}$$

and the integral representation (2.5). Thus

$$\begin{aligned} S(ka, \beta a) &= \frac{C}{\pi i} \sum_{n=-\infty}^{\infty} \int_{-\infty}^{\infty} \mathrm{e}^{\mathrm{i}\beta na + \mathrm{i}knta} \left(\lambda^{-1}(t) - \gamma^{-1}(t)\right) \mathrm{d}t \\ &= \frac{1}{4k^3 a} \sum_{n=-\infty}^{\infty} \left(\lambda_n^{-1} - \gamma_n^{-1}\right) \equiv \frac{1}{4k^3 a} \widetilde{S}(ka, \beta a), \end{aligned} \tag{4.9}$$

say, where $\widetilde{S}$ is non-dimensional and

$$\lambda_n = ((\beta_n/k)^2 - 1)^{1/2}, \quad \gamma_n = ((\beta_n/k)^2 + 1)^{1/2}, \quad \text{and} \quad \beta_n = \beta + 2n\pi/a. \tag{4.10}$$

It is convenient to define scattering angles, $\psi_n, n \in \mathbb{Z}$ by

$$\beta_n = k \cos \psi_n, \tag{4.11}$$

where $\beta_0 = \beta = k \cos \psi_0 = k \cos \psi$. Then, provided $|\beta_n| \le k$ or $|\cos \psi_n| = |\cos \psi + 2n\pi/ka| \le 1$ the ψ_n define real angles with $0 \le \psi_n \le \pi$ and such that $\lambda_n = -\mathrm{i} \sin \psi_n$. In this case we say that $n \in \mathcal{N}$. Then it is clear that the set $\mathcal{N}$ is non-empty for all ka, with at least one member corresponding to $n = 0$ and $\psi_0 = \psi$ being the incident wave angle.

So

$$\widetilde{S}(ka, \beta a) = \sum_{n \in \mathcal{N}} \left(\frac{\mathrm{i}}{\sin \psi_n} - \frac{1}{(1 + \cos^2 \psi_n)^{1/2}} \right) + \sum_{n \notin \mathcal{N}} \left(\lambda_n^{-1} - \gamma_n^{-1}\right), \tag{4.12}$$

where the infinite sum converges since $\lambda_n^{-1} - \gamma_n^{-1} \sim (ka/2n\pi)^3$ as $n \to \infty$ and the finite sum exists provided $\sin \psi_n \ne 0$ for some $n = m$, or $\psi_m = 0, \pi$, or $|\cos \psi + 2m\pi/ka| = 1$, a situation termed as resonance by Hills and Karp [11]. We shall not consider this type of resonance here.

The scattered field given by (4.5) is now

$$u_s(\mathbf{r}) = \frac{\mu(1-\mu S)^{-1}}{8\pi k^2}\sum_{n=-\infty}^{\infty}\sigma^n\int_{-\infty}^{\infty}\mathrm{e}^{\mathrm{i}k(x-na)t}\left(\frac{\mathrm{e}^{-k\lambda|y|}}{\lambda}-\frac{\mathrm{e}^{-k\gamma|y|}}{\gamma}\right)$$
$$= \frac{\mu(1-\mu S)^{-1}}{4k^3a}\sum_{n=-\infty}^{\infty}\mathrm{e}^{\mathrm{i}\beta_n x}\left(\frac{\mathrm{e}^{-k\lambda_n|y|}}{\lambda_n}-\frac{\mathrm{e}^{-k\gamma_n|y|}}{\gamma_n}\right), \tag{4.13}$$

where the Poisson formula (4.8) has been used again. The scattered field (4.13) involves plane waves arising from $n \in \mathcal{N}$ only. Thus, with $x = r\cos\theta$, $y = r\sin\theta$,

$$u_s(\mathbf{r}) \sim \frac{\mathrm{i}\mu(1-\mu S)^{-1}}{4k^3a}\sum_{n\in\mathcal{N}}\frac{\mathrm{e}^{\mathrm{i}kr\cos(\theta-\mathrm{sgn}(y)\psi_n)}}{\sin\psi_n} \tag{4.14}$$

as $r\to\infty$, arising from the first term in (4.13) for $n\in\mathcal{N}$. It follows that

$$u(\mathbf{r}) \sim \mathrm{e}^{\mathrm{i}k(x\cos\psi+y\sin\psi)} + \sum_{n\in\mathcal{N}} R_n\mathrm{e}^{\mathrm{i}k(x\cos\psi_n-y\sin\psi_n)}, \quad y\to-\infty, \tag{4.15}$$

whilst

$$u(\mathbf{r}) \sim \sum_{n\in\mathcal{N}} T_n\mathrm{e}^{\mathrm{i}k(x\cos\psi_n+y\sin\psi_n)}, \quad y\to\infty, \tag{4.16}$$

where R_n, T_n represent the non-dimensional coefficients for plane waves reflected and transmitted (respectively) from the periodic array, given by

$$R_n = \frac{\mathrm{i}\mu(1-\mu S)^{-1}}{4k^3a\sin\psi_n}, \quad \text{and} \quad T_n = \delta_{n0} + R_n. \tag{4.17}$$

Provided μ defined by (2.12) is real, conservation of mean energy flux requires that

$$\sum_{n=-\infty}^{\infty}\left(|R_n|^2+|T_n|^2\right)\sin\psi_n = \sin\psi. \tag{4.18}$$

It is possible to prove that this relation holds for μ real.

A remarkable feature of the results is the possibility of total reflection of the given incident wave by a suitably spaced array of points (see Fig. 3(a, b)). We have, using dimensionless variables, $\mu = (4k^4a^2)\widetilde{\mu} - (4/a^2)\widetilde{\kappa}$ and $\widetilde{S} = 4k^3aS$,

$$R_0 = \frac{\mathrm{i}[ka\widetilde{\mu} - \widetilde{\kappa}/(ka)^3]}{(1-[ka\widetilde{\mu}-\widetilde{\kappa}/(ka)^3]\widetilde{S})\sin\psi} \tag{4.19}$$

and we shall assume just one scattered wave so that ka satisfies $|\cos\psi \pm 2\pi/ka| > 1$. Then

$$\widetilde{S} = \widetilde{S}_r + \mathrm{i}/\sin\psi \quad \text{where } \widetilde{S}_r = \sum_{\substack{n=-\infty\\ \neq 0}}^{\infty}\left(\lambda_n^{-1}-\gamma_n^{-1}\right) - (1+\cos^2\psi)^{-1/2} \tag{4.20}$$

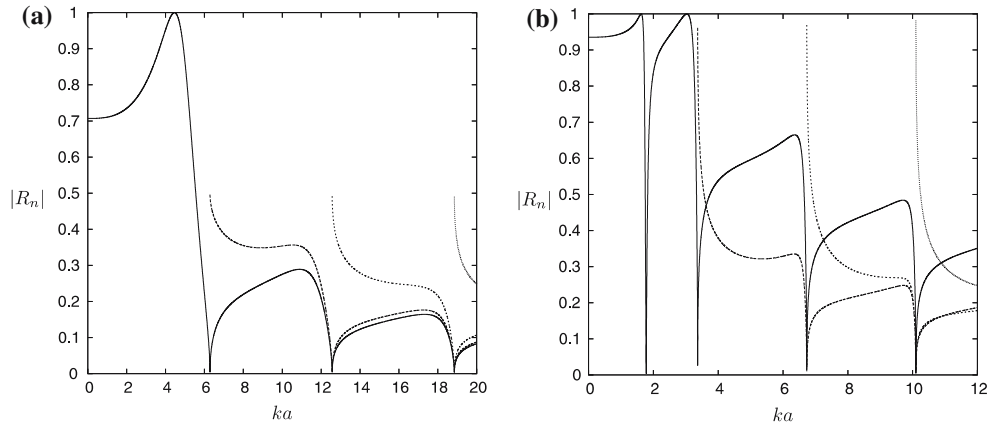

Fig. 3 Variations of reflected wave coefficients $|R_n|$ with ka for: (**a**) $\psi = 90°$ and $\widetilde{\mu}^{-1} = 0, \widetilde{\kappa} = 0$ (head incidence, pinned points) and (**b**) $\psi = 30°$ and $\widetilde{\mu} = 2, \widetilde{\kappa} = 20$ (oblique incidence, mass/spring loaded points)

and so

$$R_0 = \left[-1 - \mathrm{i}\sin\psi\left([ka\widetilde{\mu} - \widetilde{\kappa}/(ka)^3]^{-1} - \widetilde{S}_r\right)\right]^{-1} \tag{4.21}$$

is such that $R_0 = -1$ provided

$$\widetilde{S}_r = [ka\widetilde{\mu} - \widetilde{\kappa}/(ka)^3]^{-1}. \tag{4.22}$$

If $R_0 = -1$ then $T_0 = 0$ and no transmission of wave energy is possible. It is easy to see that (4.22) is satisfied for any choice of $\widetilde{\mu}$ and $\widetilde{\kappa}$ and any choice of $\psi \neq 0, \pi$. Choose without loss of generality $\cos\psi \geq 0$ so that $0 \leq \psi < \frac{1}{2}\pi$. Then as ka increases from zero to its maximum allowed value (to ensure only one reflection and transmitted wave exists) of $2\pi/(1 + \cos\psi)$ the right-hand side of (4.22) varies continuously from either zero or infinity (depending upon whether $\widetilde{\kappa} = 0$) to some finite number whose value is not important. At the same time, consideration of the term λ_{-1}^{-1} in the series part of $\widetilde{S}_r$ in (4.20) shows that $\widetilde{S}_r$ increases from the negative value of $-(1 + \cos^2\psi)^{-1/2}$ to positive infinity. It follows that there exists (at least) one value of ka for any fixed $\widetilde{\mu}, \widetilde{\kappa}$ and ψ for which (4.22) is satisfied and the incident wave is totally reflected. This result still holds when $\widetilde{\mu}^{-1} = 0$ (or $\widetilde{\kappa} \to \infty$) corresponding to pinned points since the condition (4.22) is simply $\widetilde{S}_r = 0$ and clearly the argument for the existence of a value of ka satisfying this condition remains intact.

Other features of this problem can be investigated. Thus, as $ka \to 0$, when only one reflected and transmitted mode exists, (4.21) shows that for $\widetilde{\kappa} \neq 0$, or for $\widetilde{\kappa} = 0$ and $\widetilde{\mu}^{-1} = 0$,

$$R_0 \sim \frac{-\mathrm{i}}{\mathrm{i} - \sin\psi/(1 + \cos^2\psi)^{1/2}}.$$

as $ka \to 0$. In the particular case when $\widetilde{\kappa} = 0$ and $\widetilde{\mu}$ is finite, it is equally simple to show that $R_0 \to 0$ as $ka \to 0$.

5 Trapped waves for two parallel arrays of points

As we have already observed, an interesting feature of the previous problem is that there exists a particular frequency below the first cut-off frequency (i.e., only one reflected and transmitted wave exists) at which

all the incident wave energy is reflected from the array. This property has been shown to be true for all incident wave angles, ψ and values of $\widetilde{\mu}$ and $\widetilde{\kappa}$ although the particular value of ka for which $T_0 = 0$ varies with these parameters. This leads us to the interesting prospect that, for two parallel periodic arrays of constrained points, separated by a distance to be determined, may 'trap' waves by continual reflections in each array in the absence of an incident wave. This principle has formed the basis of a number of recent studies into the phenomenon of wave-trapping in surface water waves and acoustics, where the trapped wave is said to occur 'in the continuous spectrum', since wave propagation to infinity is possible (in contrast to the next section on Rayleigh–Bloch waves). See for example [12], where it is shown that the spacing, $2b$, between the arrays should approximately satisfy $\chi = \frac{1}{2}n\pi + kb\sin\psi, n \subset \mathbb{Z}$, where, at total reflection, $R_0 = \mathrm{e}^{2\mathrm{i}\chi}$ and in this case we have shown $R_0 = -1$ so that $\chi = \pm\frac{1}{2}\pi$.

We write

$$u(\mathbf{r}) = \sum_{n=-\infty}^{\infty} A_n g(\mathbf{r}; na, b) + \sum_{n=-\infty}^{\infty} B_n g(\mathbf{r}; na, -b) \tag{5.1}$$

and assume $A_n = \sigma^n A_0$, $B_n = \sigma^n B_0$, for $\beta = k\cos\psi$, so that the phase relation between corresponding points is as though an incident wave were present even though this is not the case.

There are now two possible trapped wave types, the first which is symmetric about $y = 0$ for which we $A_n = B_n$ and the second of which is antisymmetric about $y = 0$ and where we assume $A_n = -B_n$. Following the preceding method for the single array provides the following conditions for symmetric and antisymmetric trapped waves

$$\widetilde{S}^{s,a} = [ka\widetilde{\mu} - \widetilde{\kappa}/(ka)^3]^{-1}, \tag{5.2}$$

where

$$\widetilde{S}^{s,a} = \widetilde{S}_r^{s,a} + \frac{\mathrm{i}(1 \pm \mathrm{e}^{2ikb\sin\psi})}{\sin\psi} \tag{5.3}$$

with

$$\widetilde{S}_r^{s,a} = \sum_{\substack{n=-\infty \\ \neq 0}}^{\infty} \left(\frac{(1 \pm \mathrm{e}^{-2\lambda_n kb})}{\lambda_n} - \frac{(1 \pm \mathrm{e}^{-2\gamma_n kb})}{\gamma_n} \right) - \frac{(1 \pm \mathrm{e}^{-2kb(1+\cos^2\psi)^{1/2}})}{(1+\cos^2\psi)^{1/2}} \tag{5.4}$$

and the superscripts $s(a)$ correspond to the $+(-)$ signs and refer to symmetric (antisymmetric) motions. In order to satisfy (5.2) it is necessary (but not sufficient) that $\widetilde{S}^{s,a}$ is real, whence

$$kb\sin\psi = \begin{cases} (m - \frac{1}{2})\pi, & \text{for symmetric waves} \\ m\pi, & \text{for antisymmetric waves} \end{cases}, \tag{5.5}$$

which happens to be exact agreement with the approximate formula discussed earlier (it is not difficult to see why this is so). With these values imposed we have

$$\widetilde{S}^{s,a} = \widetilde{S}_r^{s,a} \sim \widetilde{S}_r \tag{5.6}$$

for large kb, where $\widetilde{S}_r$ given by (4.20) and the condition (5.2) reduces to (4.21) which is known to be satisfied by a value of ka below the first cut-off. Similar arguments can be used to show that (5.2) can be satisfied

by a value of a/b such that ka is below the first cut-off with kb already fixed by (5.5). The result holds for $\widetilde{\mu}^{-1} = 0$ which corresponds to pinned points and the required conditions are $\widetilde{S}_r^{s,a} = 0$ with (5.5).

The full solution is given by (5.1) with $A_n = B_n = \sigma^n A_0$ or $A_n = -B_n = \sigma^n A_0$ for trapped waves symmetric or antisymmetric (respectively) about the line of symmetry, $y = 0$. Satisfying the conditions (5.3) and (5.5) for a trapped wave, ensures that there are no waves radiated as $|y| \to \infty$ and it follows that for the symmetric wave in $|y| < b$

$$u^s(\mathbf{r}) = A_0 \sum_{n=-\infty}^{\infty} \mathrm{e}^{\mathrm{i}\beta_n x} \left(\frac{\mathrm{e}^{-k\lambda_n b} \cosh k\lambda_n y}{\lambda_n} - \frac{\mathrm{e}^{-k\gamma_n b} \cosh k\gamma_n y}{\gamma_n} \right), \tag{5.7}$$

whilst for an antisymmetric wave in $|y| < b$

$$u^a(\mathbf{r}) = A_0 \sum_{n=-\infty}^{\infty} \mathrm{e}^{\mathrm{i}\beta_n x} \left(\frac{\mathrm{e}^{-k\lambda_n b} \sinh k\lambda_n y}{\lambda_n} - \frac{\mathrm{e}^{-k\gamma_n b} \sinh k\gamma_n y}{\gamma_n} \right), \tag{5.8}$$

where $\beta_n = k\cos\psi + 2\pi n/a$ and A_0 is an arbitrary multiplicative constant. It is rare to have such an explicit expression for trapped waves as given by (5.7), (5.8).

The conditions to be satisfied for a trapped modes between two rows of periodic points are (5.5) which ensures no radiated waves as $|y| \to \infty$ and (5.2) with (5.4). We thus have three independent parameters, ψ, kb and b/a but it proves useful to illustrate results using the parameter $\beta a = ka\cos\psi$ also.

Numerical results are presented in Fig. 4(a, b) for waves trapped between a pair of periodic arrays of points. In the first figure $\widetilde{\mu}^{-1} = 0$ (pinned) and in the second figure $\widetilde{\mu} = 1, \widetilde{\kappa} = 0$ (unsprung mass-loaded points). In each case the solid curves represent the values of ka as a function of $\beta a = ka\cos\psi$ whilst the dashed curves are values of b/a measured on the same vertical scale as ka and corresponding to those values of ka. The dotted diagonal lines show the boundary of the region of $(ka, \beta a)$ parameter space being considered. When $\beta a = 0$, $\psi = \frac{1}{2}\pi$ and the intersection of the solid curves with the diagonal cut-off $ka = \beta a$ represents $\psi = 0$. The lowest dashed and solid curves are for mode number $m = 1$ (the fundamental symmetric wave), increasing values of m giving rise to raised curves. Note how little the curve of ka varies with different values of m. It can be seen that the curves of ka against βa tend quickly towards a fixed curve which corresponds to the values at which $T_0 = 0$ for each ψ in the problem of scattering by a single array of points. We have limited the sequence of dashed curves to just the first four modes; two symmetric interlaced by antisymmetric modes. The sequence continues indefinitely for increasing values of b/a.

6 Rayleigh–Bloch waves along infinite periodic arrays of points

In the theory of scattering by diffraction gratings there exists the possibility of localised waves travelling along the grating in the absence of an incident wave. These are termed Rayleigh–Bloch waves by Wilcox [13, Sect. 1].

For a general diffraction grating it is not easy to determine the dominant wavenumber β modulating the periodicity of the grating but for the simpler form of the periodic array problem being considered here, progress can easily be made.

We seek a displacement $u(\mathbf{r})$ which exists in isolation, for a particular relation between a dominant wavenumber β and the infinite plate wavenumber k, for each a. Thus we assume that

$$u(\mathbf{r}) = \sum_{n=-\infty}^{\infty} A_n g(x, y; na, 0), \tag{6.1}$$

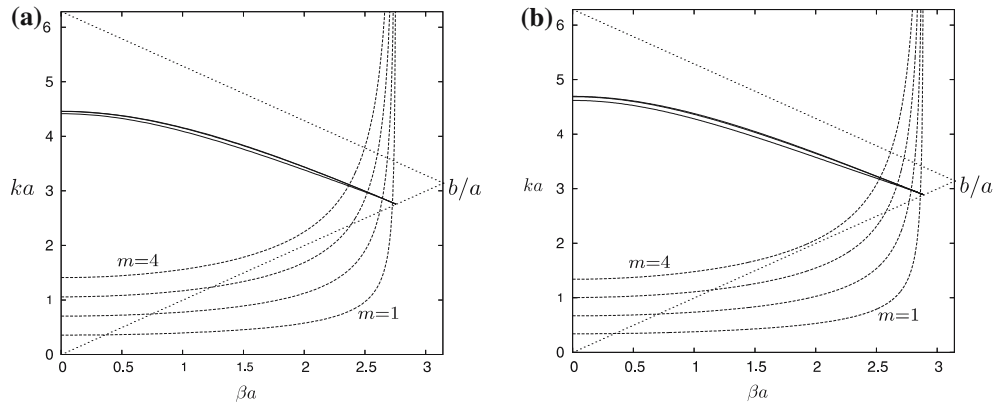

Fig. 4 Solid curves show variation of ka against βa at which trapped waves occur for a double array with (**a**) $\widetilde{\mu}^{-1} = 0$ (pinned points) and (**b**) $\widetilde{\mu} = 1, \widetilde{\kappa} = 0$ (unsprung mass loaded points); dashed curves give corresponding values of b/a against βa

where, as before $A_n = A_0\sigma^n$ but now $\beta > k$ so that there can be no incident or reflected and transmitted waves. Then

$$u(\mathbf{r}) = A_0 \sum_{n=-\infty}^{\infty} \sigma^n g(x, y; na, 0), \tag{6.2}$$

where A_0 is an arbitrary 'amplitude' factor. Applying (4.1) now gives, after relabelling the sums,

$$1 = \mu S \tag{6.3}$$

with $S(ka, \beta a)$ given by (4.9), as the condition for a solution of the form (6.2) where now S is real-valued since $\beta > k$.

It is easy to show that it is necessary to consider only values of $\beta a \in [0, \pi)$ since $S(ka, 2m\pi + \beta a) = S(ka, \beta a)$, a simple relabelling of the sum in (4.9) gives the same value for S. In addition, the relation $S(ka, 2\pi - \beta a) = S(ka, \beta a)$ can also be shown with relative ease.

In terms of non-dimensional quantities already introduced, (6.3) becomes

$$\widetilde{S} = [ka\widetilde{\mu} - \widetilde{\kappa}/(ka)^3]^{-1} \tag{6.4}$$

and now $\widetilde{S}$, as defined by (4.9), takes the range of real values between zero and infinity as ka is increased from zero to βa a fact that needs to be kept in mind during the arguments that follow in determining if solutions of (6.4) exist. Thus, a variety of situations can arise depending upon the choice of constraint at the points along the array.

First, if the points are all pinned, corresponding to $\widetilde{\mu}^{-1} = 0$ or $\widetilde{\kappa}^{-1} = 0$ then (6.4) has no solution for real $ka > 0$, and no Rayleigh–Bloch waves can exist.

Similarly, there are no solutions if $\widetilde{\mu} = 0$ and $\widetilde{\kappa} > 0$ corresponding to purely sprung points. If, on the other hand, $\widetilde{\kappa} = 0$ and $\widetilde{\mu} > 0$, corresponding to unsprung mass loaded points then its easy to see that a solution must always exist.

In the most complicated case where both $\widetilde{\mu}$ and $\widetilde{\kappa}$ are non-zero and finite the situation is less clearcut. Thus, one can show by inspecting the relation (6.4) that a solution exists if $\widetilde{\kappa}/\widetilde{\mu} < (\beta a)^4 \leq \pi^4$ for any given non-dimensional value of βa. This is because as $ka \to 0$, the right-hand side of (6.4) tends to zero, but from below. However, if the quantity in the square brackets passes through zero, as ka is increased from zero to its maximum allowed value of βa, then the right-hand side of (6.4) switches from negative to positive

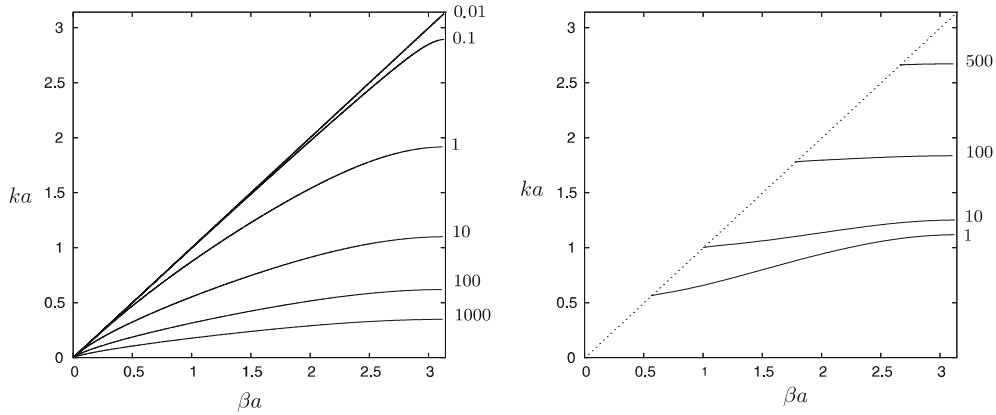

Fig. 5 Dispersion curves, ka against βa, for $\widetilde{S}(ka,\beta a)=[ka\widetilde{\mu}-\widetilde{\kappa}/(ka)^3]^{-1}$ for: (**a**) fixed $\widetilde{\kappa}=0$ and varying values of $\widetilde{\mu}$ (shown against curves); (**b**) fixed $\widetilde{\mu}=10$ and varying values of $\widetilde{\kappa}$ (shown against curves)

values and hence a solution will exist. What has been shown is that Rayleigh–Bloch solutions only exist for of values of βa satisfying $(\widetilde{\kappa}/\widetilde{\mu})^{1/4}<\beta a\le\pi$ whilst no solution exists if $\widetilde{\kappa}>\pi^4\widetilde{\mu}$.

Computations of (6.3) are given in Fig. 5(a) when $\widetilde{\kappa}=0$ where it is shown that for each positive value of $\widetilde{\mu}$, there is precisely one value of ka corresponding to each value of $\beta a\in(0,\pi]$, with $k\sim\beta$ as $\widetilde{\mu}\to 0$ and $k\to 0$ as $\widetilde{\mu}\to\infty$.

In Fig. 5(b) we choose a fixed positive value of $\widetilde{\mu}=10$ and vary $\widetilde{\kappa}$ to illustrate the theory above that Rayleigh–Bloch modes will exist provided $\widetilde{\kappa}$ does not exceed a value of $10\pi^4\approx 974$, and that for increasing values of $\widetilde{\kappa}$ solutions are predicted over a shrinking interval of values of βa.

The form of the Rayleigh–Bloch wave when (6.3) is satisfied is more clearly illustrated by applying the Poisson formula to (6.2). Thus

$$u(\mathbf{r})=\frac{A_0\mathrm{e}^{\mathrm{i}\beta x}}{4k^3a}\sum_{n=-\infty}^{\infty}\mathrm{e}^{2\pi\mathrm{i}nx/a}\left(\frac{\mathrm{e}^{-k\lambda_n|y|}}{\lambda_n}-\frac{\mathrm{e}^{-k\gamma_n|y|}}{\gamma_n}\right) \tag{6.5}$$

and $u(ma,0)=A_0\sigma^mS=A_m/\mu$ as required by (4.1). A special case arises if $\beta=\pi/a$ when (6.5) reduces to

$$u(\mathbf{r})=\frac{A_0}{2k^3a}\sum_{n=0}^{\infty}\cos[\pi(2n+1)x/a]\left(\frac{\mathrm{e}^{-k\lambda_n|y|}}{\lambda_n}-\frac{\mathrm{e}^{-k\gamma_n|y|}}{\gamma_n}\right) \tag{6.6}$$

and the displacement is now a standing wave with nodes at $x=\pm ma/2$, $m\in\mathbb{Z}$ for all y, which decays exponentially to zero with increasing $|y|$. If we restrict ourselves to $|x|<a/2$ we have a simply supported elastic strip in $|x|\le a/2$, $-\infty<y<\infty$ satisfying $u(\pm a/2,y)=u_{xx}(\pm a/2,y)=0$ in the centre of which a point mass at the origin is undergoing undamped harmonic oscillations satisfying $u(0,0)=S=1/\mu$. This is the kind of dynamic trapped mode as sought by McIver [14] in which the body (in this case a point) oscillates freely without radiation to infinity.

The effect of the presence of a Rayleigh–Bloch wave for an *infinite* periodic array upon the scattering of plane incident waves by a *finite* periodic array can be significant, as illustrated in Fig. 6. In this figure where $\widetilde{\mu}=1$ implies that the points are free to oscillate, the amplitude of every other point along an array of $N=20$ points is plotted as a function of ka. It can be observed that points undergo their maximum oscillation at a common value of $ka=1.9078$ and that, at this wavenumber, the maximum amplitude occurs at the centre of the array. The near-resonant value of ka is closely related to the value of ka at

which a Rayleigh–Bloch wave occurs with $\beta a = \pi$. This particular value of βa is significant in that it is the value for which the Rayleigh–Bloch waves take the form of standing waves—see the earlier discussion surrounding (6.6). Similar observations have been made by Maniar and Newman [2] in connection with surface water-wave interaction with long finite periodic arrays of vertical circular cylinders. There, the maximum amplification in wave elevation occurs in the vicinity of the central cylinders in the array at a frequency very close to the frequency at which standing Rayleigh–Bloch waves occur.

As an example of the type of motion on the plate at near resonance, we observe in Fig. 7 the case of oblique wave incidence at a particular instant in time; light and dark shading represents peaks and troughs on the plate.

7 An elastic plate floating on water

All of the previous problems considered in this paper can be repeated for the case of a thin elastic plate floating on water of constant depth, h, say, simply by the replacement of the Green function defined by (2.2) for the elastic plate in *vacuo* by an appropriate Green function, describing the coupling between the plate and the water. Thus we shall demonstrate that the displacement of the plate previously given by (2.1) is modified to include a term on the right hand side which relates to the pressure difference across the plate due to the presence of the water.

According to classical linear water-wave theory there exists a velocity potential $\Phi(\mathbf{r}, z, t)$ where the fluid velocity vector is given by $\mathbf{v}(\mathbf{r}, z, t) = \nabla\Phi$. Assuming a time-harmonic response of angular frequency ω and writing $\Phi(\mathbf{r}, z, t) = \Re\mathrm{e}\{\phi(\mathbf{r}, z)\mathrm{e}^{-\mathrm{i}\omega t}\}$ where, in the body of the water, Laplace's equation is satisfied,

$$\left(\Delta + \partial^2/\partial z^2\right)\phi = 0, \quad -h < z < 0, \ -\infty < x, y < \infty$$

with

$$\partial\phi/\partial z|_{z=-h} = 0$$

describing no-flow through the bed. The linearised kinematic condition on the boundary between the elastic plate, having displacement $\Re\mathrm{e}\{u(\mathbf{r})\mathrm{e}^{-\mathrm{i}\omega t}\}$, and the fluid is

$$\partial\phi/\partial z|_{z=0} = -\mathrm{i}\omega u(\mathbf{r}). \tag{7.1}$$

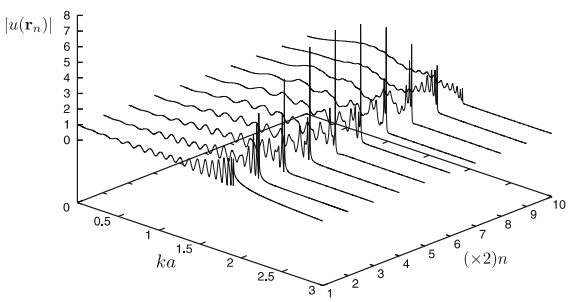

Fig. 6 The non-dimensional amplitude of mass-loaded points as a function of ka and pin number for $\psi = 0°$, $N = 20$ points and with $\widetilde{\mu} = 1, \widetilde{\kappa} = 0$

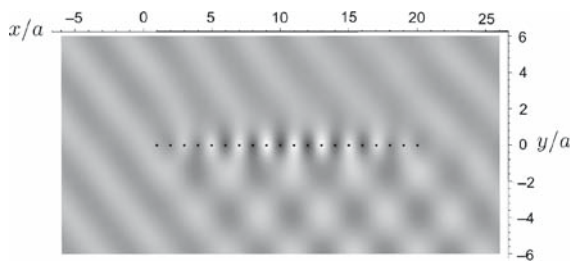

Fig. 7 Snapshot in time of the wave amplitude (light to dark represent peaks to troughs) on a plate with $\psi = 45°$, $N = 20$ mass-loaded points (shown as dots), $\widetilde{\mu} = 1, \widetilde{\kappa} = 0$ and at resonant frequency $ka = 1.9078$. Maximum amplitude at centre of array is 8 times the incident wave amplitude

The equation of motion of the plate assuming time-harmonic variations is given by

$$(D\Delta^2 - m\omega^2)u(\mathbf{r}) = [p]_{z=0} = \mathrm{i}\rho\omega\phi(\mathbf{r},0) - \rho g u(\mathbf{r}), \tag{7.2}$$

where $[p]_{z=0}$ denotes the jump in the pressure across the plate whose value is determined using Bernoulli's linearised equation for the pressure in the fluid. In the above, ρ is the water density and g is gravitational acceleration. Rearrangement of (7.2) into a form consistent with Sect. 2 gives

$$(\Delta^2 + \mathcal{M} - k^4)u(\mathbf{r}) - \mathrm{i}\omega^{-1}\mathcal{F}\phi(\mathbf{r},0) = 0, \tag{7.3}$$

where $k^4 = m\omega^2/D$ as before and $\mathcal{M} = \rho g/D$, $\mathcal{F} = \rho\omega^2/D$.

For an elastic plate of thickness d over water, $\mathcal{M}/k^4 = \rho g/\rho_p d\omega^2$ where ρ_p is the density of the plate. Using typical values, $d = 1$, $\rho_p \approx \rho$, $g = 10$ shows that $\mathcal{M}/k^4 \approx 10/\omega^2$. For wavelengths between 40 m and 180 m, ω varies between about $3\,\mathrm{s}^{-1}$ and $0.5\,\mathrm{s}^{-1}$ corresponding to wave periods between 3 s and 12 s. So, only for unrealistically high-frequency short-wavelength waves $k^4 \gg \mathcal{M}$, whilst for longer waves of lower frequency in the range of physical interest, $k^4 \ll \mathcal{M}$. In the former of the two scenarios, $\mathcal{M}$ can effectively be neglected whilst $\mathcal{F}$ can also be shown to have a relatively small contribution and the wave motion is dominated by flexural effects. Thus, the results already obtained for the elastic plate in *vacuo* will be representative of those for these high-frequency motions over water. In the more realistic case of longer waves, the situation is reversed and the effects of fluid loading dominate inertia forces.

A flexural-gravity incident wave propagating on a homogeneous elastic plate at an angle ψ to the positive x-axis over water is described by the potential

$$\phi_i(\mathbf{r},z) = A\mathrm{e}^{\mathrm{i}k_0(x\cos\psi + y\sin\psi)}\cosh k_0(z+h),$$

where $A = -\mathrm{i}\omega/(k_0\sinh k_0 h)$ and from (7.1), the plate displacement is given by

$$u_i(\mathbf{r}) = \mathrm{e}^{\mathrm{i}k_0(x\cos\psi + y\sin\psi)}. \tag{7.4}$$

Here, k_0 is the wavenumber (replacing k for an elastic plate in *vacuo*) and is determined as the real positive root, $\gamma = k_0$, of the dispersion relation

$$K(\gamma) \equiv (\gamma^4 + \mathcal{M} - k^4)\gamma\sinh\gamma h - \mathcal{F}\cosh\gamma h = 0. \tag{7.5}$$

We note that there are also an infinite series of pure imaginary roots to (7.5) above, $\gamma = \pm k_m$, $m = 1,2,\ldots$ ordered such that $\Im\mathrm{m}\{k_{m+1}\} > \Im\mathrm{m}\{k_m\} > 0$. In addition there are four complex roots, labelled $\gamma = \pm k_{-1}$ and $\gamma = \pm k_{-2}$ such that $k_{-1} = p + \mathrm{i}q$, with $p, q > 0$, and $k_{-2} = -p + \mathrm{i}q$ both exist in the upper half plane.

We define a fundamental Green function $G(\mathbf{r}, z; \mathbf{r}')$ for a source in the elastic plate over water satisfying

$$\left(\Delta + \partial^2/\partial z^2\right)G = 0, \quad -h < z < 0, \ -\infty < x, y < \infty \tag{7.6}$$

with $G_z|_{z=-h} = 0$, and

$$(\Delta^2 + \mathcal{M} - k^4)g_w - \mathrm{i}\omega^{-1}\mathcal{F}G|_{z=0} = \delta(\mathbf{r} - \mathbf{r}') \tag{7.7}$$

the resulting plate elevation given by

$$g_w(\mathbf{r};\mathbf{r}') = \frac{\mathrm{i}}{\omega}G_z|_{z=0}. \tag{7.8}$$

Fox and Chung [15] have previosuly derived the Green function which, in the current notation is given by

$$G(\mathbf{r}, z; \mathbf{r}') = \frac{\omega}{4} \sum_{m=-2}^{\infty} \frac{Y_m(z) Y_m'(0)}{C_m} H_0(k_m \rho)$$

and consequently

$$g_w(\mathbf{r}; \mathbf{r}') = \frac{\mathrm{i}}{4} \sum_{m=-2}^{\infty} \frac{[Y_m'(0)]^2}{C_m} H_0(k_m \rho), \tag{7.9}$$

where $Y_m(z) = \cosh k_m(z + h)$ and C_m is given by (A.2). We note the asymptotic expansion of the Hankel function, $H_0(z)$, for small arguments,

$$H_0(k_m \rho) = \text{const} + \frac{2\mathrm{i}}{\pi} \log k_m \rho - \frac{\mathrm{i} k_m^2 \rho^2}{2\pi} \log k_m \rho + O(k_m^2 \rho^2), \qquad \rho \to 0$$

where the value of the constant is not important in what follows. Using this expansion in (7.9) along with the relations in (A.1)–(A.4) of the Appendix we can show that

$$g_w(\mathbf{r}; \mathbf{r}') \sim C_w + \frac{\rho^2 \log \rho}{8\pi} + O(\rho^2), \qquad \text{as} \quad \rho \to 0. \tag{7.10}$$

This form for the Green function in the vicinity of the point of forcing is, as expected, of the same form as (2.7) for a plate in *vacuo*, but instead of taking the value $C = \mathrm{i}/8k^2$ we now have

$$C_w = -\frac{1}{2\pi} \sum_{m=-2}^{\infty} \frac{[Y_m'(0)]^2}{C_m} \log k_m. \tag{7.11}$$

With the appropriate Green function given by (7.9) constructed and the property (7.10) with C_w now given by (7.11) established we can approach each of the problems previously considered for a plate in *vacuo* with little extra complication. For example, for the scattering of waves by N points located at $\mathbf{r}_n$, $n = 1, \ldots, N$ on the elastic plate on water constrained by a mass/spring system, we simply write

$$\phi(\mathbf{r}, z) = \phi_i(\mathbf{r}, z) + \sum_{n=1}^{N} A_n G(\mathbf{r}, z; \mathbf{r}_n)$$

with associated displacements

$$u(\mathbf{r}) = u_i(\mathbf{r}) + \sum_{n=1}^{N} A_n g_w(\mathbf{r}; \mathbf{r}_n).$$

This equation is the same form as (3.1) and the procedure used for a plate in *vacuo* follows exactly as described in Sect. 3.

For problems involving infinite periodic arrays considered in Sects. 4–6, the procedure for an elastic plate over water follows in exactly the same manner, but we must replace S by

$$S_w = \sum_{n=-\infty}^{\infty} \sigma^{-n} g_w(na, 0; 0, 0).$$

As a reminder, $\sigma = \mathrm{e}^{\mathrm{i}\beta a}$, a is the spacing between adjacent points and $\beta = k \cos \psi$. Use of the integral identity for the Hankel function gives

$$S_w = \sum_{n=-\infty}^{\infty} \sigma^{-n} \frac{\mathrm{i}}{4} \sum_{m=-2}^{\infty} \frac{[Y_m'(0)]^2}{C_m} \left(\frac{1}{\pi \mathrm{i}} \int_{-\infty}^{\infty} \mathrm{e}^{\mathrm{i} k_m n a t} \lambda^{-1}(t) \mathrm{d}t \right)$$

and $\lambda(t) = (t^2 - 1)^{1/2}$ as in (2.6). Subsequent use of the Poisson summation formula (see (4.8) in Sect. 4) gives, after some algebra,

$$S_w = \frac{1}{2a} \sum_{m=-2}^{\infty} \frac{[Y'_m(0)]^2}{C_m} \sum_{n=-\infty}^{\infty} \frac{1}{(\beta_n^2 - k_m^2)^{1/2}} \tag{7.12}$$

and $\beta_n = \beta + 2n\pi/a$. In its present form the second sum is divergent. However, because of the relation (A.1), we can write

$$S_w = \frac{1}{2a} \sum_{m=-2}^{\infty} \frac{[Y'_m(0)]^2}{C_m} \sum_{n=-\infty}^{\infty} \left(\frac{1}{(\beta_n^2 - k_m^2)^{1/2}} - \frac{1}{|\beta_n|} \right),$$

the value of S_w is unchanged and the second sum is now convergent. Indeed the second series decays like $O(m^2/n^3)$ for each fixed value of m and since it can be shown [16] that the term $[Y'_m(0)]^2/C_m = O(m^{-6})$ as $m \to \infty$, the double sum converges rapidly in the form written.

Proceeding further shows how the reflection and transmission coefficients, R_n, T_n, for $n \in \mathcal{N}$ (defined in Sect. 4) can be derived from the far-field behaviour of the scattered part of the plate elevation, which works out to be

$$u_s \sim \frac{\mathrm{i}A_0}{2a} \frac{[Y'_0(0)]^2}{k_0 C_0} \sum_{n \in \mathcal{N}} \frac{\mathrm{e}^{\mathrm{i}k_0 r \cos(\theta - \mathrm{sgn}(y)\psi_n)}}{\sin \psi_n}, \quad \text{as } y \to \pm\infty$$

with $A_0 = \mu/(1 - \mu S_w)$ and where ψ_n are the scattering angles (see Sect. 4), so that

$$R_n = \frac{\mathrm{i}\mu(1 - \mu S_w)^{-1}[Y'_0(0)]^2}{2k_0 a C_0 \sin \psi_n},$$

whilst $T_n = \delta_{n0} + R_n$. It follows from consideration of the imaginary part of S_w, in the case when there is only one reflected and transmitted wave, that $R_0 = -1$ (and hence $T_0 = 0$) when the condition $\mathfrak{Re}\{S_w\} = 1/\mu$ is met. A proof that there exists a frequency for which this condition is satisfied was provided in Sect. 4 for an elastic plate in *vacuo*, when S_w is replaced by the much simpler S. The increased complexity of the expression for S_w does not allow us to make the same type of progress here. Indeed, numerical results show that only for certain ranges of parameters is there a frequency for which there is total reflection from the array (i.e., $|R_0| = 1$).

In Fig. 8 we show the maximum amplitude at the centre of four pinned points on an elastic plate over water. In this example (and later ones) we choose the plate thickness, $d = 1\,\mathrm{m}$, the effective Young's modulus $E = 5 \times 10^9\,\mathrm{Pa}$, Poisson's ratio, $\nu = 0.3$, the plate density to be $925\,\mathrm{kg\,m^{-3}}$, the density of water as $1025\,\mathrm{kg\,m^{-3}}$ and the water depth to be 20 m.

In Fig. 8 pinned points are placed at $\mathbf{r}_n = (\pm a, \pm a)$, and a/h takes the values $\frac{1}{2}$, 1 and 2 so that the points form the vertices of square with sides of length 20, 40 and 80 m respectively. Larger values of $k_0 a$ imply shorter wavelengths and so the range of values of $k_0 a$ in Fig. 8 has been restricted to $k_0 a < 5$ to remove unrealistically short wavelengths. Comparison with Fig. 1(a) appears to show an increasing agreement with the in *vacuo* results for smaller values of a/h. However, this is not surprising since a reduction in a/h implies, for each fixed value of non-dimensional quantity $k_0 a$, an increase in k_0 and hence a shortening of the wavelength. We have already argued that results for shorter wavelengths for plates over water will tend towards those for a plate in *vacuo*. For example, the curve showing the peak resonance in Fig. 8 is for $a/h = \frac{1}{2}$—or $a = 10\,\mathrm{m}$—and resonance occurs at $k_0 a = 1.63$ corresponding to a wavelength of approximately 40 m. For $a/h = 1$—or $a = 20\,\mathrm{m}$—a much smaller resonant peak occurs at a wavelength of

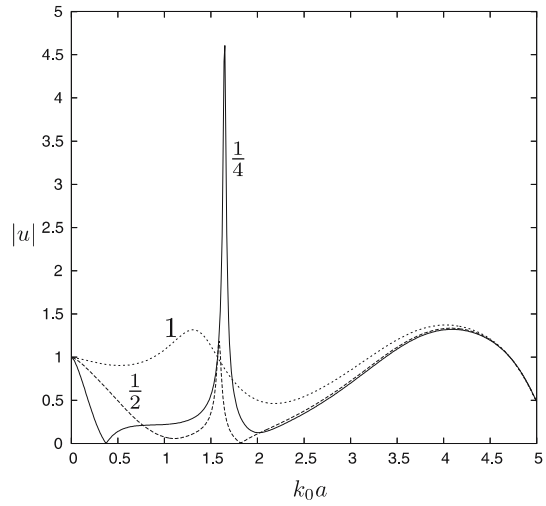

Fig. 8 Maximum displacement at the origin, $|u| = |u(0,0)|$ as ka varies for: (**a**) $N = 4$ pinned points at $(\pm a, \pm a)$ with $\psi = 0°$. The values of a/h are shown against curves

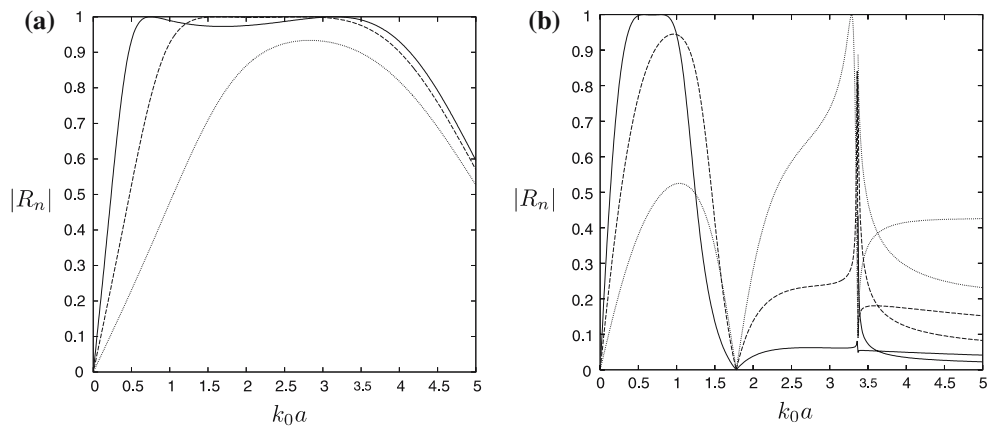

Fig. 9 Variations of reflected wave coefficients $|R_n|$ with k_0a for: (**a**) $\psi = 90°$ and $\widetilde{\mu}^{-1} = 0, \widetilde{\kappa} = 0$ (head incidence, pinned points) and (**b**) $\psi = 30°$ and $\widetilde{\mu} = 2, \widetilde{\kappa} = 20$ (oblique incidence, mass/spring loaded points). In each plot point separation distance $a = 10$ m (solid lines), $a = 20$ m (long dashed), $a = 40$ m (dotted)

approximately 80 m. In other words, the side of the square formed by the pinned points is approximately half a wavelength of the incident wave at resonance.

In Fig. 9 we show the reflected wave amplitudes for an infinite periodic array of constrained points in an elastic plate on water. We use the same set of physical parameters as before, and restrict the range of wavenumber values to $k_0a < 5$. For the sake of comparison, Figs. 9(a, b) mimic parameters chosen in producing Fig. 3(a, b) for a plate in *vacuo*. Thus, Fig. 9(a) has wave approaching a periodic array of pinned points head-on, whilst in Fig. 9(b) the wave approaches obliquely ($\psi = 30°$) and the points are constrained by a mass/spring system. In each of the two figures, results for three different array separations ($a/h = \frac{1}{2}$, 1 and 2 implies $a = 10$, 20 and 40 m) are presented. In Fig. 9(b), a second set of reflected wave 'cut-on' beyond the appropriate value of k_0a. The common value of k_0a at which $R_0 = 0$ is easily explained by the fact that $\mu = 0$ for $k_0a = (\widetilde{\kappa}/\widetilde{\mu})^{1/4}$. It also has a physical explanation, since the wave frequency corresponding to this value of k_0a exactly matches the natural frequency of oscillation for the local mass/spring system at each point, implying that the points become completely transparent to the incident wave at this frequency. It can be seen from this set of results that total reflection is possible, but, unlike the plate in *vacuo*, not guaranteed. It is also clear from these results that there can be a quite significant qualitative overall difference between the results for an in *vacuo* plate and one bounded below by a heavy fluid.

8 Conclusions

In this paper we have considered a number of problems which involve the interaction of flexural waves on a thin elastic plate which is constrained to move at a number of points via a mass/spring system. Attention has focused on elastic plates which are not bounded below by a fluid since the resulting mathematical analysis can be demonstrated in a very straightforward manner. Towards the end of the paper, we have considered the extension which involves an elastic plate floating on water, as a model of a large floating structure either tethered or supported at a number of points. In particular we have shown that the methods used in the preceding sections carry over to this more complex physical situation in a quite straightforward manner. We have drawn attention to the differences that exist between the simplified in *vacuo* problem and the problem involving fluid loading, but have also illustrated similarities in the type of results that can be obtained.

A range of interesting wave phenomena have been demonstrated, both numerically and, in many cases, assisted by analysis. These involve near resonance for finite arrays of constrained points, total wave reflection by infinite periodic arrays, trapping of waves by parallel periodic arrays and Rayleigh–Bloch waves along periodic arrays.

Appendix A: Some important identities

Evans and Porter [16] derived certain identities, which are used in Sect. 8 of this paper, and which we briefly derive here since a different notation is being used. The first identity is

$$0 = \frac{1}{2\pi \mathrm{i}} \oint_C \frac{\gamma^2 \sinh \gamma h}{K(\gamma)} \mathrm{d}\gamma = 2 \sum_{m=-2}^{\infty} \frac{k_m^2 \sinh k_m h}{K'(k_m)} = \sum_{m=-2}^{\infty} \frac{[Y'_m(0)]^2}{C_m}, \tag{A.1}$$

where $K'(k_m) = 2k_m C_m / Y'_m(0)$ and

$$C_m = \tfrac{1}{2}[\mathcal{F}h + (5k_m^4 + \mathcal{M} - k^4) \sinh^2 k_m h]. \tag{A.2}$$

The vanishing of the integral follows since the integrand is $O(\gamma^{-3})$ as $|\gamma| \to \infty$ and C represents a circular contour whose radius tends to infinity. Also, since the integrand is odd in γ, the residues from the poles at $\gamma = k_m$ double up with those from poles at $\gamma = -k_m$. Calculations based on similar principles give, first

$$0 = \frac{1}{2\pi i} \oint_C \left(\frac{\gamma^4 \sinh \gamma h}{K(\gamma)} - \frac{1}{\gamma} \right) \mathrm{d}\gamma = 2 \sum_{m=-2}^{\infty} \frac{k_m^4 \sinh k_m h}{K'(k_m)} - 1 = \sum_{m=-2}^{\infty} \frac{k_m^2 [Y'_m(0)]^2}{C_m} - 1, \tag{A.3}$$

the extra term in the integrand being included to ensure sufficient decay at infinity and, then,

$$0 = \frac{1}{2\pi i} \oint_C \left(\frac{\gamma^6 \sinh \gamma h}{K(\gamma)} - \gamma \right) \mathrm{d}\gamma = 2 \sum_{m=-2}^{\infty} \frac{k_m^6 \sinh k_m h}{K'(k_m)} = \sum_{m=-2}^{\infty} \frac{k_m^4 [Y'_m(0)]^2}{C_m}. \tag{A.4}$$

References

1. Eatock Taylor R (ed) (2003) The third international conference on hydroelasticity in marine technology. Oxford, UK
2. Maniar HD, Newman JN (1997) Wave diffraction by a long array of cylinders. J Fluid Mech 339:309–329
3. Callan M, Linton CM, Evans DV (1991) Trapped modes in two-dimensional waveguides. J Fluid Mech 229:51–64
4. Evans DV, Porter R (1997) Trapped modes about multiple cylinders in a channel. J Fluid Mech 339:331–356
5. Evans DV, Porter R (1997) Near-trapping of water waves by circular arrays of vertical cylinders. Appl Ocean Res 19:83–89

6. Ziman JM (1972) Principles of the theory of solids. Cambridge University Press, Cambridge
7. Evans DV (1981) Power from water waves. Ann Rev Fluid Mech 13:157–187
8. Evans DV, Meylan MH (2005) Scattering of flexural waves by a pinned thin, elastic sheet floating on water. In: The 20th international workshop on water waves and floating bodies, Longyearbyen, Svalbard.
9. Norris AN, Vermula C (1995) Scattering of flexural waves on thin plates. J Sound Vib 181(1):115–125
10. Newman JN (1977) Marine hydrodynamics. M.I.T. Press
11. Hills NL, Karp SN (1965) Semi-infinite diffraction gratings – I. Comm Pure Appl Maths 18:203–233
12. Porter R (2002) Trapping of water waves by pairs of submerged cylinders. Proc R Soc London A 458:607–624
13. Wilcox CH (1984) Scattering theory for diffraction gratings, Applied mathematical sciences, vol 46, Springer
14. McIver P (2005) Are there trapped modes in the water-wave problem for a freely-floating structure? In: The 20th international workshop on water waves and floating bodies. Longyearbyen, Svalbard
15. Fox C, Chung H (1998) Green's function for forcing of a thin floating plate. Number 408, Department of Mathematics Research Reports Series, University of Auckland
16. Evans DV, Porter R (2003) Wave scattering by narrow cracks in ice sheets floating on water of finite depth. J Fluid Mech 484:143–165